Journal of Alloys and Compounds 500 (2010) 247–251

Contents lists available at ScienceDirect

Journal of Alloys and Compounds

journal homepage: www.elsevier.com/locate/jallcom

# Electrocatalytic activity of Pt doped $TiO_2$ nanotubes catalysts for glucose determination

Xiao Han, Yihua Zhu*, Xiaoling Yang, Chunzhong Li*

*Key Laboratory for Ultrafine Materials of Ministry of Education, School of Materials Science and Engineering, East China University of Science and Technology, Shanghai 200237, China*

ARTICLE INFO

*Article history:*
Received 24 November 2009
Received in revised form 31 March 2010
Accepted 1 April 2010
Available online 10 April 2010

*Keywords:*
Semiconductors
$TiO_2$
Nanotube
Glucose oxidase
Glucose biosensor

ABSTRACT

A hybrid system of titanium dioxide nanotubes (TNTs) incorporated with poly(amidoamine) dendrimers-encapsulated platinum nanoparticles (Pt-DENs) was constructed in a neutral aqueous solution through electrostatic interaction. The TNTs/Pt-DENs nanohybrids immobilized glucose oxidase (GOx) was used to modify a glassy carbon electrode (GCE) for detecting the electrocatalytic response to the reduction of glucose. The structures of nanohybrids were characterized by TEM, XRD and FT-IR, the performance of modified electrodes was characterized by cyclic voltammetry (CV) and amerometric measurements, respectively. The modified electrodes, which had a fast response of glucose oxidase less than 3 s, could be used for the determination of glucose oxidase ranging from 2 μM to 12 mM. The detection limits were 1 μM at signal-to-noise ratio of 3.



## 1. Introduction

The direct electrochemistry of enzymes has received increasing attention in the last few years, which provide a platform for fabricating new kinds of mediator free biosensors, battery application and biomedical devices [1,2]. However, enzymes exhibit a rather slow rate of heterogeneous electron-transfer at conventional electrodes, because of the deep burying of the electroactive prosthetic groups, the unfavorable orientations of enzymes at electrodes [3]. Therefore, the studies are focusing on selecting ideal electrode materials, such as carbon nanotubes [4], iron oxide nanoparticles [5–7] and biomaterials [8–10] to enhance the direct electron-transfer between the enzymes and underlying electrodes.

Since various $TiO_2$ nanostructures which have favorable physical optical and electrical properties have been reported in the last few years. Much attention has been given to the study of structural characteristics, properties, and applications [11,12]. $TiO_2$ nanotubes, owing to their large length–diameter ratio, continue to be involved in bioelectrochemistry field due to their chemical inertness, rigidity, nontoxicity, high hydrophilicity and good biocompatibility [13–18]. However, a common problem occurred when using metal oxide semiconductors to modify electrodes is poor charge transport [19–21].

Metal nanoparticles such as Au [22], Ti (III) [18], Ag [23], and Pt [24] were introduced to dope with $TiO_2$ nanotubes to overcome the deficiency mentioned above. These kinds of metal nanoparticles have excellent conductivity, catalytic property and biocompatibility. They can perform as "electronic wires" to enhance the electron-transfer between redox centers in enzymes and electrode surfaces, and as catalysts to increase electrochemical reactions [25–28]. However, these nanoparticles are intended to agglomerate, it is necessary to use protective agents, such as small organic molecules or polymers to prevent aggregation. Highly branched dendritic macromolecules poly (amidoamine) (PAMAM) could be used to modify electrode surface due to their good biocompatibility and adequate functional groups for chemical fixation [29]. It was reported that the dendrimers were capable of increasing the concentration of hydrophobic molecules at the electrode–solution interface, improving the sensitivity as well as the selectivity of certain specific electrochemical reactions [30].

Therefore, our main concern in the present work is to enhance the conductivity and sensitivity of TNTs, and further the direct electron-transfer of glucose oxidase. In order to improve the conductivity and sensitivity of TNTs, Pt-DENs nanoparticles were used to dope with TNTs, then the TNTs/Pt-DENs were loaded with the model protein, glucose oxidase (GOx). The TNTs/Pt-DENs/GOx biosensor could be obtained by immersing TNTs/Pt-DENs composites in the GOx-contained buffer solution. Much better conductivity to the resultant TNTs/Pt-DENs/GOx biosensor can be achieved attributing to the doping treatment. Direct electrochemistry of GOx has been observed. The biosensor further exhibits fine

* Corresponding authors. Fax: +86 21 64250624.
*E-mail addresses:* yhzhu@ecust.edu.cn (Y. Zhu), czli@ecust.edu.cn (C. Li).

0925-8388/$ – see front matter © 2010 Elsevier B.V. All rights reserved.
doi:10.1016/j.jallcom.2010.04.019

bioelectrocatalytic characteristic of fast response, high sensitivity for the amperometric detection of glucose.

## 2. Experimental

### 2.1. Materials

Glucose oxidase (GOx, EC.1.1.3.4, TYPEVII, 150 U/mg) was purchased from Fluka, which was modified by the periodate-oxidized GOx ($IO_4$-GOx) according to the literature [31]. And glucose was from Sigma–Aldrich. Pt-DENs were synthesized according to the previous literature [32]. Phosphate buffer solutions (PBS, 0.1 M) with various pH values were prepared by mixing stock standard solutions of $Na_2HPO_4$ and $NaH_2PO_4$, and adjusting the pH with $H_3PO_4$ or NaOH. Doubly distilled and deionized water was used through this work.

### 2.2. Preparation of TNTs

Titanate nanotubes were synthesized by hydrothermal method using commercial $TiO_2$ nanoparticles powder (P25, Degussa, Germany) as a starting material. A conversion from nanoparticles to nanotubes was achieved by treating the nanoparticle powder with 10 M NaOH at different temperatures, for 24 h, in the autoclave. The precipitates were neutralized thoroughly with distilled water for 5 times, soaked with 1 M NaOH for 10 h, then filtered and dried at atmospheric condition. The detailed procedure is reported elsewhere [33,34].

### 2.3. Preparation of Pt-DENs/TNTs/GOx nanocomposites

0.3 g $TiO_2$ nanotubes (TNTs) was dispersed in 10 mL of a Pt-DENs colloid solution (pH 7) and shaked for 1 h. The result solution was centrifuged at a speed of 6000 rpm to get the product of Pt-DENs/TNTs hybrid materials. The hybrid material (10 mg) prepared above was dispersed in a solution of GOx (20 mg/mL, pH 6) and shaken for 1 h for enzyme absorption. The bioconjugates were then centrifuged and washed with distilled water three times.

### 2.4. Preparation of Pt-DENs/TNTs/GOx biosensor

Glass carbon (GC, 3 mm diameter, Model CHI 104, CH Instruments) electrodes were polished with 1.0, 0.3 and 0.05 mm alumina powder, respectively, then cleaned in a piranha solution (a 1:3 mixture of 30% $H_2O_2$ and concentrated $H_2SO_4$) and finally sonicated thoroughly in double distilled water. Next, the polished electrode was sonicated in acetone and doubly distilled water and then allowed to dry at room temperature. Then, 5 μL of the Pt-DENs/TNTs/GOx bioconjugates prepared above this suspension colloid was deposited on the surface of the pretreated GCE. The electrode was then left to dry and was stored for at least 24 h at 4 °C. The biosensor was stored under the same conditions when not in use. The TNTs or Pt-DENs modified GCE were fabricated using the same GCE by the same method.

### 2.5. Characterization

Morphology and microstructure of the synthesized materials were examined by Transmission electron microscopy (TEM, JEOL HF-2010 TEM), FT-IR (Nicolet AVATAR360) and X-ray Diffract meter (RIGAKU, D/MAX 2550 VB/PC). All electrochemical experiments were performed on a CHI 660A electrochemical workstation (CH Instru. Co., Shanghai, China) at 20 °C (±2) °C. The working electrode was a modified GCE. A saturated calomel electrode (SCE) served as reference electrode, and a Pt wire served as counter electrode. The working solutions were deoxygenated with nitrogen gas for 15 min before measurement and a nitrogen atmosphere was maintained over the solutions during experiment.

## 3. Results and discussion

### 3.1. Structural characteristic of TNTs and Pt-DENs/TNTs composite

Fig. 1 is a typical X-ray diffraction (XRD) data taken from the $TiO_2$ nanotube samples. The strong diffraction peak at $2\theta$ angles of 25.0°, 37.4° and 48.5° may correspond to the spacing of (1 0 1), (0 0 4) and (2 0 0) of the anatase (tetragonal) phase, two diffraction peaks at $2\theta$ angles of 27.4°, 36.3° may correspond to the spacing of (1 1 1), (1 0 1) of the rutile phase. Because the nanotubes may form by rolling up the two-dimensional sheets of $TiO_2$ structure, some diffraction peaks of rutile phase $TiO_2$ may not appear in the XRD pattern [35,36].

FT-IR spectrum of TNTs is shown in Fig. 2. Some bands can be observed: at 3390 $cm^{-1}$, assigned to the stretching of a hydroxyl group that was chemisorbed on a surface defect site, and

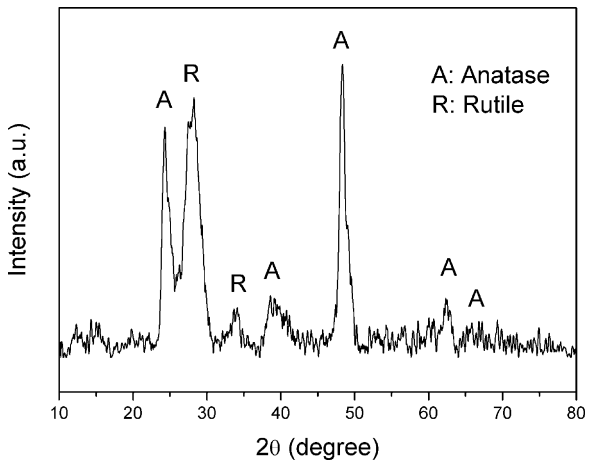


**Fig. 1.** XRD pattern of $TiO_2$ nanotube.

1623 $cm^{-1}$, pertaining to H–O–H bending for molecular water. The absorption band at 1380 $cm^{-1}$ represents the symmetric bending of $CH_3$ groups. These groups can help the conjunction and dispersion of Pt-DENs nanoparticles. The band at 500 $cm^{-1}$ was associated with the Ti–O–Ti stretching mode of $TiO_2$ [37].

Partially quarternized poly (amidoamine) (PAMAM) dendrimers having both quaternary ammonium groups and primary amines can be used as a polymeric template reservoir to prepare stable platinum–dendrimer nanocomposites. It was found that the resulting nanocomposites remain stable for several months. As shown in Fig. 3b, TEM image showed that well-defined nanosized platinum nanoparticles were almost monodispersed, with average particle diameter of ca. 3 nm and narrow size distribution. The inset of Fig. 3b also showed a high-magnification TEM image of a single Pt nanoparticle and the single crystal structure was observed. Similar results have been reported in the literate [32,38]. Fig. 3a illustrated that the as-prepared TNTs have nearly uniform diameters of around 10 nm and nanotube walls of around 5 nm. It can be seen from Fig. 3b that Pt-DENs nanoparticles on TNTs surface were slightly flattened with sizes in the range of 2–3 nm. The modification of Pt-DENs with positively charged could be easily attracted onto TNTs through electrostatic interaction in aqueous and form the TNTs/Pt-DENs composite.

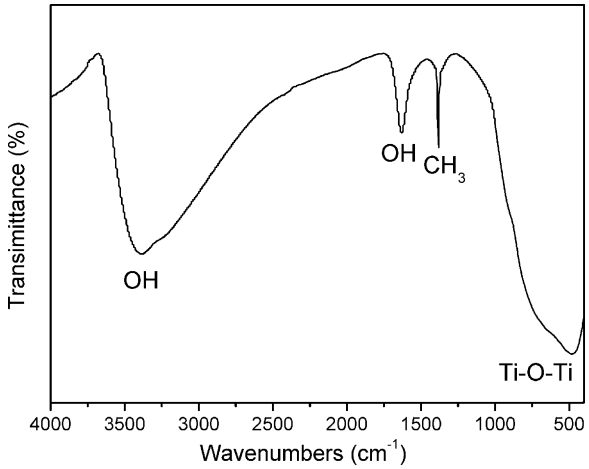


**Fig. 2.** FT-IR spectrum of $TiO_2$ nanotube.

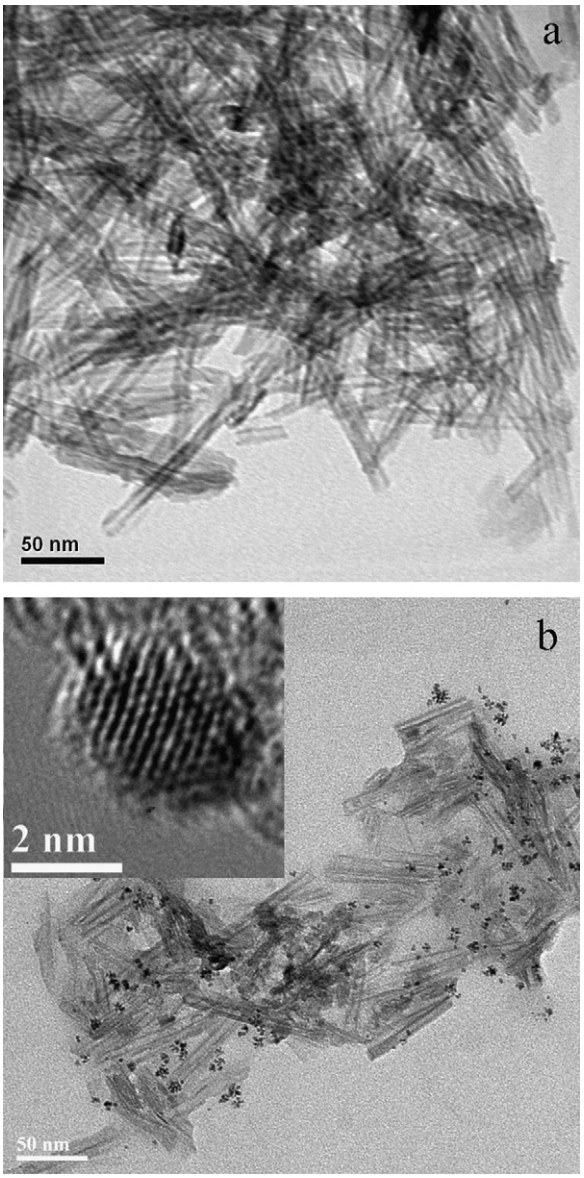


**Fig. 3.** The TEM images of $TiO_2$ nanotube (a), and Pt-DENs/TNTs (b). The inset is a high-magnification TEM image of Pt-DENs.

### 3.2. Electrochemical activity of TNTs and Pt-DENs/TNTs

The electrochemical activities of TNTs and Pt-DENs/TNTs were characterized by electrochemical impedance spectroscopy (EIS) using 5.0 mM $[Fe(CN)6]^{4-/3-}$ as the marker ions at their formal potential in 0.10 M KCl solutions. The measured complex impedance ($Z$) versus frequency, known as Nyquist Plot is shown in Fig. 4. Well-defined frequency-dependent semicircle impedance curves were observed at the high frequency range followed by a straight line. Charge transfer resistance, $R_{ct}$, determines the diameter of the semicircle. The diameter of the semicircle for Pt-DENs/TNTs was much smaller than that for TNTs, indicating that Pt-DENs/TNTs modified GCE has much higher conductivity than that of TNT modified GCE. Pt-DENs/TNTs modified GCE also showed smaller semicircle in Fig. 4 than Pt-DENs modified GCE, which indicated that Pt-DENs/TNTs modified GCE has best conductivity among these electrodes.

The direct electrochemistry behavior of GOx on both TNTs and Pt-DENs/TNTs was studied. Fig. 5 showed CVs obtained from the TNTs, TNTs/GOx, Pt-DENs, Pt-DENs/GOx, Pt-DENs/TNTs and

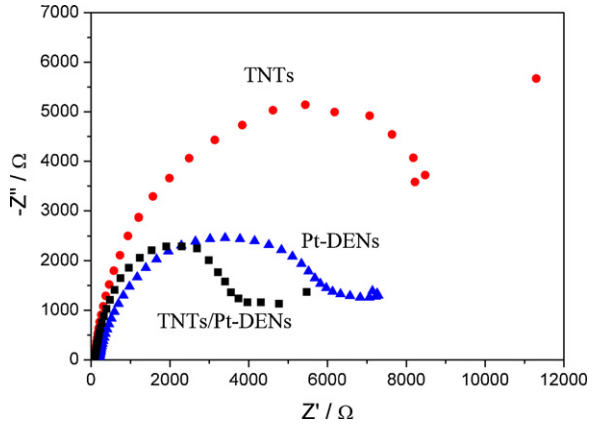


**Fig. 4.** EIS of Pt-DENs, TNTs and Pt-DENs/TNTs modified GCE in 0.10 M KCl solutions with 5.0 mM $[Fe(CN)6]^{4-/3-}$.

Pt-DENs/TNTs/GOx modified GCEs in pH 6.8 deoxygenated PBS. There was no reaction peak current observed for TNTs, Pt-DENs or Pt-DENs/TNTs modified GCEs within the potential window. However, reaction peaks for both TNTs/GOx and Pt-DENs/TNTs/GOx were easily observed in Fig. 5a, b and c, respectively. The Pt-DENs/TNTs/GOx has much higher reversibility of direct electrochemistry than the TNTs/GOx and Pt-DENs/GOx in terms of its much more prominent redox peak current and more symmetric redox wave. The peak-to-peak separation was 90 mV at scan rate 100 mV/s, which was smaller than 200 mV for GOx in Polypyrole film [39] and 300 mV for GOx in carbon nanotubes [40] observed at the same scan rate, indicating more reversible behavior for faster electron-transfer of GOx than the reported literatures can be achieved.

The isoelectric point, $I_p$ of GOx is 4.5, and therefore at pH > $I_p$, it is net negatively charged, while at pH < $I_p$, it is positively charged. During the preparation of the TNTs/Pt-DENs/GOx composite modified electrode, GOx was used as a negatively charged material for preparing the bioconjugates. Besides, the cathodic peak current of TNTs/Pt-DENs/GOx showed strong dependence on the pH of external solution. When solution pH changed from 5.0 to 9.0, Fig. 6 showed the maximum response current value can be observed at pH 6.8. So a pH 6.8 of 0.1 M phosphate buffer was used to support electrolyte for glucose detection in most cases.

### 3.3. Electrocatalysis of GOx in TNTs and Pt-DENs/TNTs

The amperometric responses of the Pt-DENs/GOx, TNTs/GOx and Pt-DENs/TNTs composite modified GC electrode upon the successive additions of glucose to 0.10 M pH 7.0 PBS at an applied potential of −0.35 V were shown in Fig. 7. The Pt-DENs or TNTs modified GC electrode showed a much smaller response to glucose than that of the Pt-DENs/TNTs modified GC electrode at the same glucose concentration. The linearity of Pt-DENs/GOx, TNTs/GOx and Pt-DENs/TNTs/GOx were 0.25–2 mM, 0.05–5 mM and 10 μM to 12 mM, respectively, with a signal-to-noise ratio of 3, respectively. The sensitivities of the three modified electrodes were 10.3 $\mu A\,mM^{-1}\,cm^{-2}$, 29.03 $\mu A\,mM^{-1}\,cm^{-2}$, 43.6 $\mu A\,mM^{-1}\,cm^{-2}$, respectively. This indicated that Pt-DENs/TNTs/GOx has better response and performance toward the glucose than TNTs/GOx and Pt-DENs/GOx. The mechanism might be Pt-DENs/TNTs/GOx have larger surface area compared to Pt-DENs/GOx, which would provided a favorable microenvironment for the entrapped GOx. Besides, sensitivity of Pt-DENs/TNTs/GOx is higher than that of TNTs/GOx, because Pt-DENs acting as “electrical wires” do enhance electron-transfer between the GOx and modified electrode.

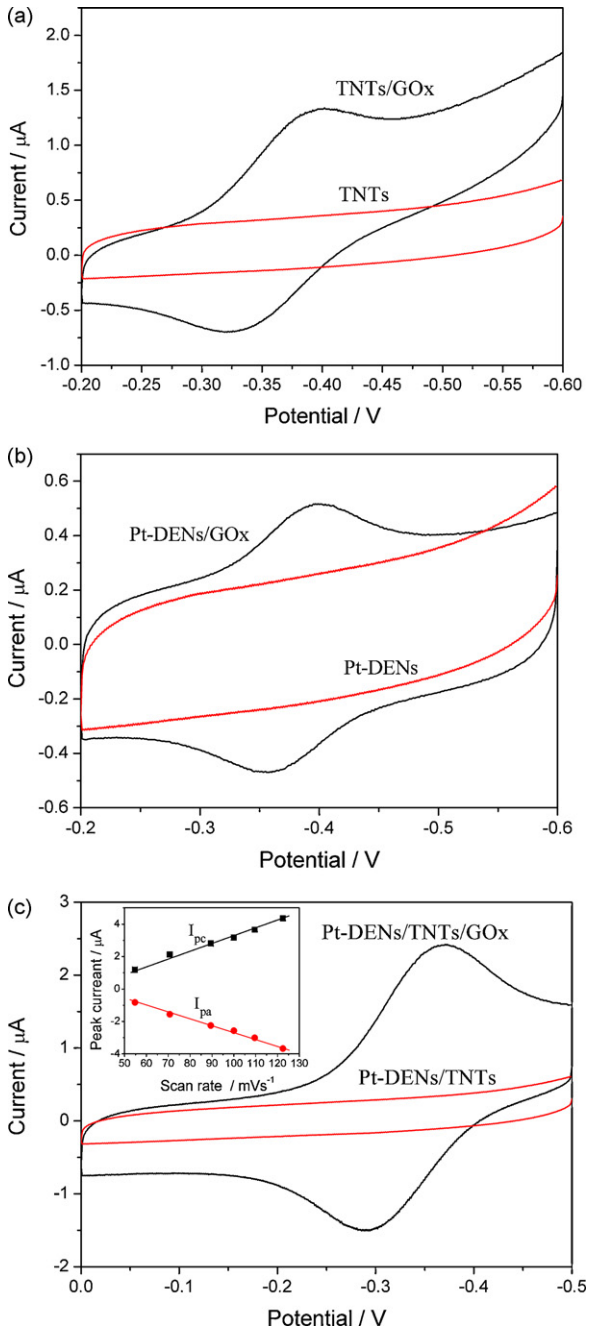


**Fig. 5.** CVs of (a) TNTs and TNTs/GOx modified GCEs, (b) Pt-DENs and Pt-DENs/GOx, (c) Pt-DENs/TNTs and Pt-DENs/TNTs/GOx modified GCEs in 0.1 M pH 6.8 PBS solutions at 100 mV/s, and inset of (b) is the plot of anodic and cathodic peak currents of Pt-DENs/TNTs/GOx electrode versus different the scan rate.

Moreover, the electrocatalytic current of the Pt-DENs/TNTs/GOx modified GCE increases clearly with each addition of glucose to the solution. The current reached its maximum value within 3 s after each addition of glucose, which suggested that the Pt-DENs/TNTs/GOx modified GCE can respond rapidly to the change of the concentration of glucose. Thus, the Pt-DENs/TNTs/GOx modified GCE showed an excellent electrocatalytic response to the reduction of glucose. The detection limit of the Pt-DENs/TNTs/GOx biosensor is 1 μM at a signal-to-noise ratio of 3, which is better to others' reports [39,40]. These results indicated that the GOx entrapped in the Pt-DENs/TNTs composite possesses electrocatalytic activity to glucose. The stability of the biosensor was further studied in the linear range of glucose. When the glucose

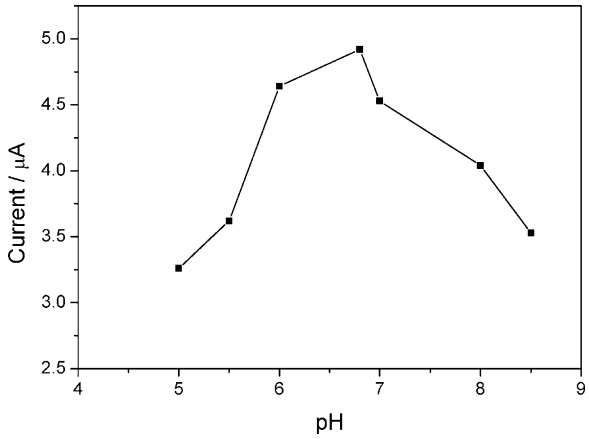


**Fig. 6.** Plot of peak current versus pH value.

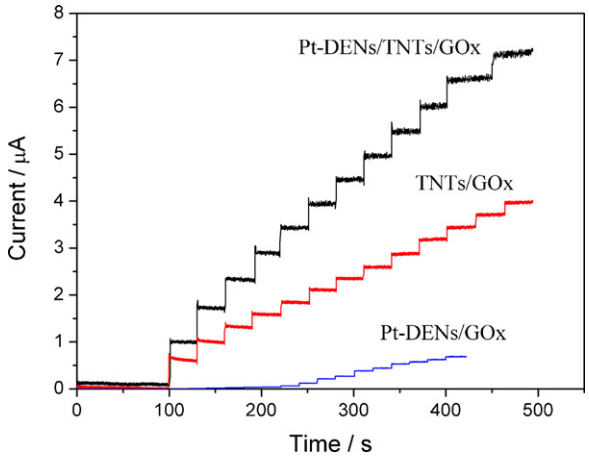


**Fig. 7.** Current–time curve of the Pt-DENs/GOx, TNTs/GOx and Pt-DENs/TNTs/GOx measured with an increase of 15 μmol $L^{-1}$ in the glucose concentration of glucose in 0.1 M PBS at −0.35 V.

biosensor has been stored in a 0.1 M PBS for 3 weeks at 4 °C, the biosensor retains over 90% response of its initial sensitivity to the reduction of glucose, demonstrating its good long-term stability.

## 4. Conclusions

In this paper, we reported preparation of the Pt-DENs/TNTs composite and immobilization of GOx onto the GC electrode. The immobilized GOx retained its biological activity well and shows high catalytic activity to the reduction of glucose. Under the optimized experimental conditions, the catalytic currents were linear to the concentrations of glucose in the ranges of 2 μM to 12 mM and the corresponding detection limits are 1 μM (S/N = 3). The sensor showed a good reproducibility and stability. The fabrication method of biosensor opens a new opportunity for the development of simple and reliable other enzymes.

## Acknowledgements

This work was supported by the National Natural Science Foundation of China (20925621, 20976054), the Key Project of Science and Technology for Ministry of Education (107045), the Innovation Program of Shanghai Municipal Education Commission (09ZZ58), the Program of Shanghai Subject Chief Scientist (08XD1401500), the Shuguang Scholar-Tracking Foundation of Shanghai (08GG09),

and the Shanghai Leading Academic Discipline Project (project number: B502).

## References

[1] Q.L. Sheng, J.B. Zheng, X.D. Shang-Guan, W.H. Lin, Y.Y. Li, R.X. Liu, Electrochim. Acta 55 (2010) 3185–3191.
[2] Z. Durmus, H. Kavas, M.S. Toprak, A. Baykal, T.G. Altınçekiç, A. Aslan, A. Bozkurt, S. Coşgun, J. Alloys Compd. 484 (2009) 371–376.
[3] H. Xu, H. Dai, G. Chen, Talanta 81 (2010) 334–338.
[4] H. Yin, Y. Zhou, J. Xu, S. Ai, L. Cui, L. Zhu, Anal. Chim. Acta 659 (2010) 144–150.
[5] L.Q. Yang, X.L. Ren, F.Q. Tang, L. Zhang, Biosens. Bioelectron. 25 (2009) 889–895.
[6] T.T. Baby, S. Ramaprabhu, Talanta 80 (2010) 2016–2022.
[7] D.L. Zhao, X.X. Wang, X.W. Zeng, Q.S. Xia, J.T. Tang, J. Alloys Compd. 477 (2009) 739–743.
[8] C. Liu, X. Guo, H. Cui, R. Yuan, J. Mol. Catal. B-Enzym. 60 (2009) 151–156.
[9] J.P. Hervás Pérez, E. López-Cabarcos, B. López-Ruiz, Talanta, doi:10.1016/j.talanta.2010.02.010.
[10] W.C. Shih, M.C. Yang, M.S. Lin, Biosens. Bioelectron. 24 (2009) 1679–1684.
[11] J. Wang, Z. Wang, H. Li, Y. Cui, Y. Du, J. Alloys Compd. 494 (2010) 372–377.
[12] G. Li, F. Liu, Z. Zhang, J. Alloys Compd. 493 (2010) L1–L7.
[13] H. Yang, C. Pan, J. Alloys Compd. 492 (2010) L33–L35.
[14] S. Sreekantan, L.C. Wei, J. Alloys Compd. 490 (2010) 436–442.
[15] Y.F. Tu, S.Y. Huang, J.P. Sang, X.W. Zou, J. Alloys Compd. 482 (2009) 382–387.
[16] M.W. Xiao, L.S. Wang, X.J. Huang, Y.D. Wu, Z. Dan, J. Alloys Compd. 470 (2009) 486–491.
[17] X.Y. Pang, D.M. He, S.L. Luo, Q.Y. Cai, Sens. Actuators B 137 (2009) 134–138.
[18] M. Liu, G. Zhao, K. Zhao, X. Tong, Y. Tang, Electrochem. Commun. 11 (2009) 1397–1400.
[19] W. Huang, S. Gao, X. Ding, L. Jiang, M. Wei, J. Alloys Compd. 495 (2010) 185–188.
[20] Z. Gu, X.Y. Chen, Q.D. Shen, H.X. Ge, H.H. Xu, Polymer 15 (2010) 902–907.
[21] W. Zhang, T. Yang, C. Yin, G. Li, K. Jiao, Electrochem. Commun. 11 (2009) 783–786.
[22] P. Benvenuto, A.K.M. Kafi, A. Chen, J. Electroanal. Chem. 627 (2009) 76–81.
[23] D. Fang, K.L. Huang, S.Q. Liu, Z.J. Li, J. Alloys Compd. 464 (2008) L5–L9.
[24] X. Pang, D. He, S. Luo, Q. Cai, Sens. Actuators B 137 (2009) 134–138.
[25] Y. Fu, Z.D. Wei, S.G. Chen, L. Li, Y.C. Feng, Y.Q. Wang, X.L. Ma, M.J. Liao, P.K. Shen, S.P. Jiang, J. Power Sources 189 (2009) 982–987.
[26] W. Ngeontae, W. Janrungroatsakul, P. Maneewattanapinyo, S. Ekgasit, W. Aeungmaitrepirom, T. Tuntulani, Sens. Actuators B 137 (2009) 320–326.
[27] P. Santhosh, K.M. Manesh, S. Uthayakumar, S. Komathi, A.I. Gopalan, K.P. Lee, Bioelectrochemistry 75 (2009) 61–66.
[28] J. Lin, C. He, Y. Zhao, S. Zhang, Sens. Actuators B 137 (2009) 768–773.
[29] Y. Qu, Q. Sun, F. Xiao, G. Shi, L. Jin, Bioelectrochemistry 77 (2010) 139–144.
[30] Q. Chen, S. Ai, X. Zhu, H. Yin, Q. Ma, Y. Qiu, Biosens. Bioelectron. 24 (2009) 2991–2996.
[31] M. Zhao, R. Crooks, Angew. Chem. Int. Ed. Engl. 38 (1999) 364–366.
[32] H. Zhu, Y. Zhu, X. Yang, C. Li, Chem. Lett. 35 (2006) 326–328.
[33] T. Kasuga, M. Hiramatsu, A. Hoson, T. Sekino, K. Niihara, Langmuir 14 (1998) 3160–3163.
[34] Y.F. Chen, C.Y. Lee, M.Y. Yeng, H.T. Chiu, Mater. Chem. Phys. 81 (2003) 39–44.
[35] J.M. Macak, S. Aldabergerova, A. Ghicov, P. Schmuki, Phys. Stat. Sol. A 203 (2006) R67–R69.
[36] J. Zhao, X. Wang, T. Sun, L. Li, Nanotechnology 10 (2005) 2450–2454.
[37] M.D. Lu, S.M. Yang, J. Colloid Interface Sci. 333 (2009) 128–134.
[38] F.N. Crespilho, V. Zucolotto, C.M.A. Brett, O.N. Oliveira, J. Phys. Chem. B 110 (2006) 17478–17483.
[39] L.H. Tang, Y.H. Zhu, L.H. Xu, X.L. Yang, C.Z. Li, Electroanalysis 19 (2007) 1677–1682.
[40] L.H. Xu, Y.H. Zhu, L.H. Tang, X.L. Yang, C.Z. Li, Electroanalysis 19 (2007) 717–722.